ЖУРНАЛ НАНО- ТА ЕЛЕКТРОННОЇ ФІЗИКИ
Том 18 № 2, 02030(5cc) (2026)

REGULAR ARTICLE

Structural and Optical Properties of ZnO Nanorods Synthesized via Tulshi (Ocimum tenuiflorum) Extract: A Green Approach

K. Barman[1,2], P. Chakraborty[2], P.K. Samanta[3,1]

[1] *Department of Physics, Sri Ramkrishna Sarada Vidya Mahapitha, Hooghly-713102, West Bengal, India*
[2] *Department of Physics, Raiganj University, Uttar Dinajpur-733134, West Bengal, India*
[3] *Department of Physics, Prabhat Kumar College, Contai-721404, Purba Medinipur, West Bengal, India*

(Received 04 August 2025; revised manuscript received 19 April 2026; published online 29 April 2026)

A simple wet-chemical method has been used to synthesized ZnO nanorods inspired from the green approach using Ocimum tenuiflorum extract. X-ray diffraction data revealed the formation of crystalline nanostructures with crystallite size ~ 18 nm. The nanorods are polycrystalline in nature and are attached together via electrostatic attraction between the charged facets of ZnO nanocrystals. Fourier transformed infrared spectra revealed the formation of Zn-O bond along with various aromatic bonds also due to the molecules of O.tenuiflorum extract. Strong UV absorption and emission was observed owing to the band edge transition of the direct band gap of 3.85 eV. Band gap enhancement is the evidence of occurrence of quantum confinement in the synthesized ZnO nanorods. The synthesized nanorods exhibit strong antimicrobial activity against E. Coli as found from the optical density measurement after bacterial incubation with the nanorods.

Keywords: Zinc-oxide, Green-synthesis, Absorption, Bandgap, Quantum-confinement.

DOI: 10.21272/jnep.18(2).02030 PACS numbers: 81.16.Ta, 03.65.Ta, 78.55.Qr

1. INTRODUCTION

Nanomaterials are in the forefront of research because of two unique properties: surface enhancement and quantum confinement [1]. Nanomaterials offer large surface to volume compared to bulk materials resulting interesting surface properties such as enhancement in catalytic activity, surface adsorption, improved sensing response, hydrophobicity, and super clean surface [2-7]. Again, due to their small size, the carriers are confined within a small volume, which changes the density of states and the electronic energy of the system. As a result, electronic, thermal, optical, and magnetic properties change significantly compared to their bulk counterpart [8]. In this context, several metals and metal oxides are widely being studied by the researchers. Quantum effect leads to surface plasmon resonance resulting interesting plasmonic properties such as size dependent colour, plasmonic oscillation associate local heating which have potential biomedical applications [9]. In semiconductors, quantum confinement leads to band gap enhancement resulting significant changes in optical emission and absorption. Among the widely studied semiconductor nanostructures, zinc oxide (ZnO) is very popular due to its high and direct band gap of 3.37 eV and large excitonic binding energy of 60 meV at room temperature [10]. This property makes ZnO a potential material for stable UV-lasing [11]. When grown at low-temperature, ZnO nanocrystals contains several defects such as vacancies, interstitials and voids [12]. These defect states have energy lower than the conduction band and therefore, lay within the band gap of ZnO. Any transition associated with these defect states give rise to visible emission from ZnO nanostructures. In addition, due to non-centrosymmetric crystal structure, a permanent dipole moment is observed in ZnO nanocrystals and gives rise to piezoelectric effect [13]. This is very useful in harvesting electrical energy from mechanical vibrations. Furthermore, due to high transparency, good electrical conductivity, surface hydrophobicity, ZnO is widely is being used in solar cells and various coating materials [12]. The major obstacle of using nanoparticles in medical application is the toxicity. However, studies revealed that nanoparticles synthesized with various leaves extract have very low toxicity and is found to be biocompatible and safe. Several researchers have reported the green synthesis of ZnO nanoparticles using various leaves extract such as neem, basak, kalmegh, and many more [14]. However, there are very few reports on the synthesis of ZnO using Tulshi (*Ocimum tenuiflorum*) leaf Extract.

Tulshi leaves have good antioxidant properties and is used to treat cold, cough and other digestive problems in Indian Ayurveda. Inspired by this Indian Knowledge System (IKS) of Medicine, we report here a simple green synthesis approach to synthesize ZnO nanostructures. Detailed structural and optical characterization were carried out to investigate the effect of size on the properties of ZnO nanostructures. Finally, the material has been tested against *E. Coli* to study its antibacterial effect.

2. EXPERIMENTAL

2.1 Material Preparation

[1] Correspondence e-mail: pijush.samanta@gmail.com

Cite this article as: K. Barman et al., *J. Nano- Electron. Phys.* 18 No 2, 02030 (2026) https://doi.org/10.21272/jnep.18(2).02030

We have followed a green approach to synthesize ZnO nanostructures. First, Tulshi leaves were collected form the local forest of Contai and washed with distilled water and ethanol and dried in sunlight for 6 h. 20 g of leaves were crushed and put in 1000 ml of water and boiled for 30 min. After cooling, the solution was filtered with Whatman No. 1 filter paper and the extract is stored in refrigerator for further use. In a standard synthesis procedure, a 0.1 M Zn^{2+} ion solution was prepared by dissolving 0.88 g of zinc acetate $[ZnCH_3(COO)_2\ 2H_2O]$ dihydrate in 40 ml of the stock extract. 40 ml of leaf extract were mixed with 1.6 g of sodium hydroxide (NaOH) to create a 1 M solution. Zinc acetate solution was added for five minutes while the NaOH solution was continuously stirred. The reaction was further carried on for 1 h. A greenish white precipitate formed at the flask's bottom at the conclusion of the reaction. For additional characterization, the precipitate was filtered, cleaned with deionized water, and dried in a furnace.

Proto A-XRD diffractometer was used to collect the X-ray diffraction (XRD) data using Cu-kα radiation (wavelength ~ 1.54 Å) with Bragg's diffraction range $30° < 2\theta° < 60°$. Surface structure of the material was analyzed in a ZEISS-MERLIN field emission scanning electron microscope (FESEM) with an operation voltage of 5 kV. Fourier-transformed infrared (FTIR) spectra was used to investigate the formation of various chemical bonds and their identification. The absorption data were obtained from a double-beam UV-visible (UV-Vis) absorption spectrophotometer (Perkin Elmer UV-vis NIR) in the range of 200-1200 nm. Room-temperature photoluminescence (PL) data were recorded using a PerkinElmer lambda spectrophotometer with a Xenon lamp as the source of excitation. The antimicrobial effect was investigated by measuring the change in optical density using an absorption spectrophotometer.

3. RESULTS AND DISCUSSIONS

Typical FESEM image of the synthesized ZnO nanostructures grown using Tulshi leaves extract is shown in Fig. 1. Thick nanorods are found to form. The length of the nanorods varies in the range of ~ 100-500 nm, while their diameters are in the range of ~ 100-200 nm. Such variation of length indicates the heterogeneous growth of the nanoparticles in the solution.

In the wet-chemical process, at the beginning of the reaction of the precursors (zinc acetate and sodium hydroxide), ZnO nuclei are formed. However, due to heterogeneous seeding, the growth of the seeds is nonuniform in size, leading to inhomogeneity in the development of the nanocrystals [16]. After formation of the nanorods, they are attached by electrostatic attraction and form thick nanorods as found in the FESEM (Fig. 1).

Typical XRD pattern of the synthesized ZnO nanorods is shown in Fig. 2. Sharp and distinct peaks are observed at 31.84°, 34.61°, 36.49°, 47.47° and 56.89° which confirms the hexagonal unit-cell structure of ZnO with Miller indices (100), (002), (0101), (102) and (110) respectively. The space group is P63mc. The sharp peaks indicate the formation of well crystalline nanoparticles.

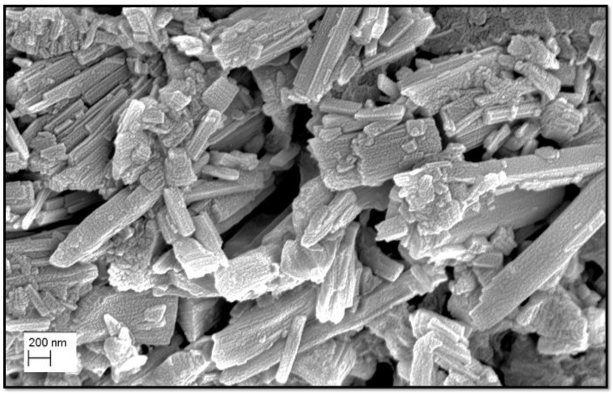

Fig. 1 – FESEM images of green synthesized ZnO nanorods

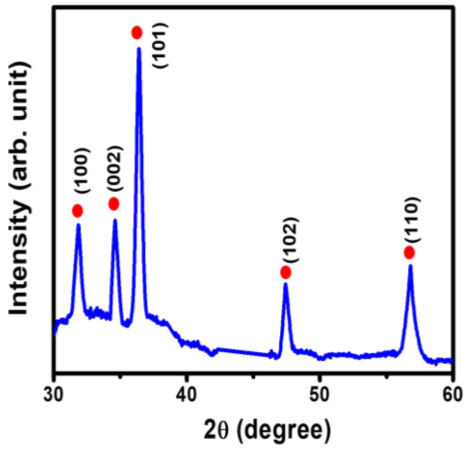

Fig. 2 – XRD pattern of the green synthesized ZnO nanorods

The crystallite size was calculated from Scherrer formula [16]:

$$D = \frac{0.89\lambda}{\beta \cos\theta} \quad (1)$$

Here, β is the full-width at half-maxima of the diffraction peak appeared at Bragg's diffraction angle 2θ and λ being the wavelength of the X-ray used in the diffraction. For this calculation we fitted the (101) peak using Gaussian function and evaluated the parameter β as can be seen in Fig. 3. The crystallite size was calculated to be 18 nm. The crystallite size is less than the diameter of the nanorods, that indicates the nanorods are composed of several crystallites, i.e. polycrystalline in nature. Small variation in peak positions was observed (see Fig. 4) caused by the lattice strain in the crystal [17].

The presence of various types of chemical bonds was analyzed using the FTIR absorption data as shown in Fig. 5. The absorption bands appearing at 481 cm^{-1} and 1108 cm^{-1} confirms the formation of ZnO and are due to stretching modes of vibration of ZnO [18]. Some water molecules may be absorbed by the material, giving rise to the O-H stretching and bending modes appearing at 1631 cm^{-1} and 3441 cm^{-1} respectively [19]. The attachment of organic molecules of Tulshi leaves extract was confirmed by the presence of C-H bending and stretching absorption band appearing at 794 cm^{-1} and 2621 cm^{-1} respectively [20].

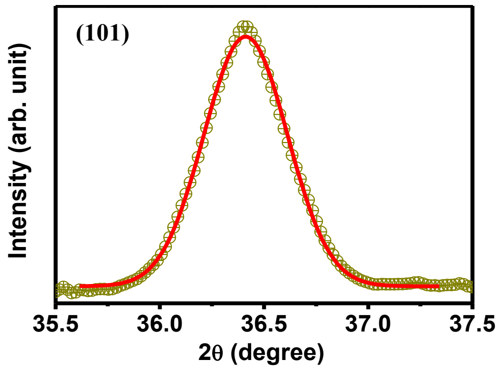

Fig. 3 – Gaussian fitting of (101) XRD peak

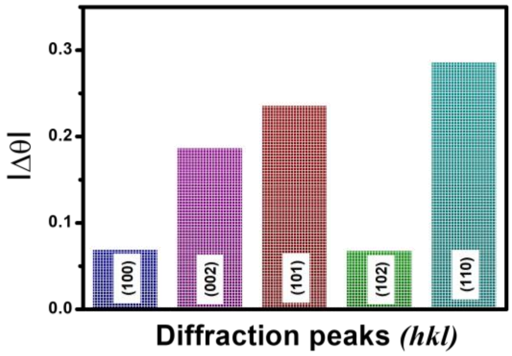

Fig. 4 – Variation of 2θ values in comparison to JCPDS data

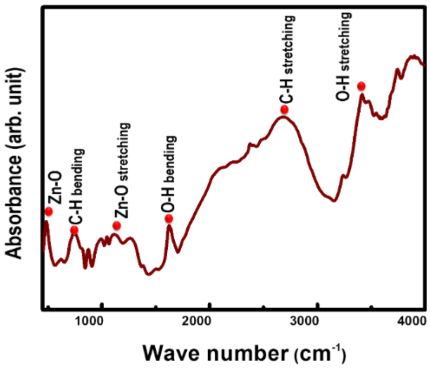

Fig. 5 – FTIR spectrum of the synthesized ZnO nanorods.

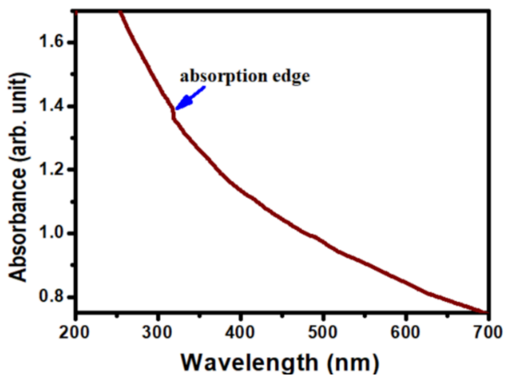

Fig. 6 – UV-Vis absorption spectrum of the ZnO nanorods

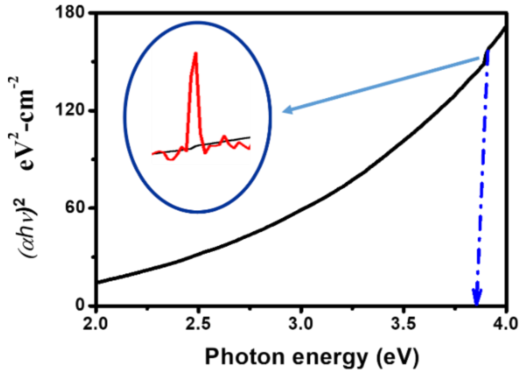

Fig. 7 – Tauc plot to estimate the band gap

Typical UV-Vis absorption spectra of the green synthesized ZnO is shown in Fig. 6. The absorption gradually decreases from UV to visible region of electromagnetic spectrum. Absorption peak appeared at 321 nm which is usually found for ZnO. This UV absorption peak is an indication of formation of ZnO nanoparticles. The band gap was calculated from the UV-Vis absorption data using Tauc equation given by [21]:

$$(\alpha h\nu)^2 = C\left(h\nu - E_g\right) \qquad (2)$$

Here, $h\nu$ is the incident photon energy, α represents the absorption coefficient, E_g corresponds to the band gap of the nanomaterials, and C is a proportionality constant. The plot of $(\alpha h\nu)^2$ against photon energy ($h\nu$) is shown in Fig. 7. According to Tauc's theory, the strong absorption leads to the appearance steep in the plot at the band gap energy. For detecting this steep position, we have differentiated the Tauc graph and shown in the inset of Fig. 7. The tangent drawn from this sharp absorption region to the $h\nu = 0$ axis, the band gap was calculated to be 3.85 eV. This band gap enhancement compared to bulk ZnO ($E_{g,bulk}$=3.37 eV) indicates the formation of ZnO nanoparticles and quantum confinement effect.

Typical room temperature photoluminescence e(PL) spectra of the green synthesized ZnO nanorods are shown in Fig. 8. Strong UV luminescence peak is observed at 326 nm.

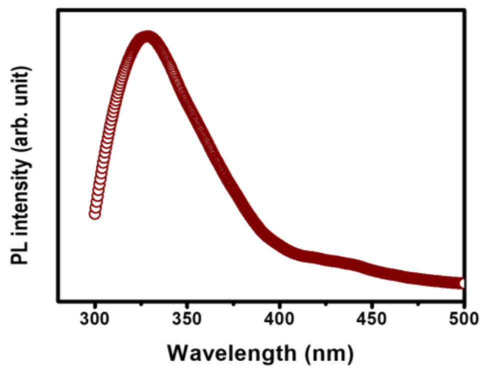

Fig. 8 – PL spectrum of synthesized ZnO nanorods

This UV peak corresponds to an energy of ~3.81 eV. This is very close to that of the band gap of determined from the absorption data which are very consistent. This PL peak in the high energy region (UV) is due to direct band-edge transition [22]. This UV emission is accompanied by a very weak visible peak at ~435 nm. In ZnO nanostructures, several defect states are developed when grown at low temperature chemical growth. These states lay in between the conduction band and valence band. Therefore, the emission peak at 435 nm is due to these shallow level defect states. [23]

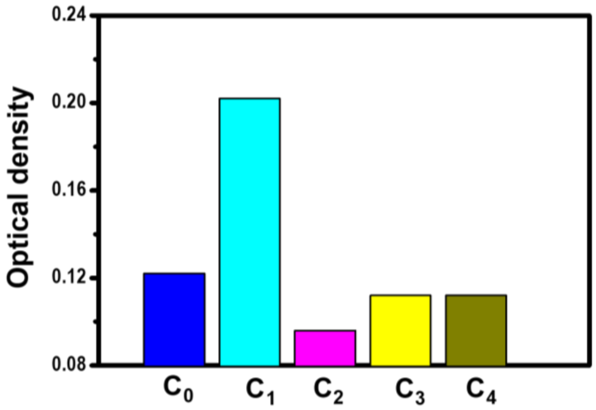

Fig. 9 – Optical density profile to study the antimicrobial effect of synthesized ZnO nanorods against *E. Coli*.

The antimicrobial activity of the green synthesized ZnO nanorods was investigated by studying the optical density. Each well of a 96-well plate with a flat bottom received 100 μL of nutritional broth. After that, 100 μL of the solution was added to the first column of the first row, and 100 μL was removed from the first well in order to add the next well vertically. Similarly, up until the fourth well, the same procedure was followed for this column. The nutrient and bacterial wells were combined after 10 μL of bacterial sample (0.5 McFaraland standard) was added equally to each well. Following the wells' incubation at 37 °C, a 24-hour optical density reading at 620 nm was obtained, along with a zero-time optical density measurement. The result is shown in Fig. 9. It can be seen that compared to the standard references (C_0), the first dilution (C_1) shows more activity compared to other three dilutions (C_2, C_3, and C_4). Therefore, the green synthesized can be used as an antibacterial agent against *E. Coli*.

4. CONCLUSIONS

In conclusion, a simple wet-chemical method has been successfully deployed to synthesize ZnO nanorods aided with Tulshi leaves extract. Well crystalline nanorods were observed which are found to agglomerated due to surface-charge interaction. Presence of Zn-O stretching mode was confirmed from the FTIR spectrum which also confirms the presence of various aromatic compounds of Tulshi present in the sample. The small crystallite size leads to quantum confinement as evident from the UV-Vis absorption spectrum. The band gap enhancement also supports the occurrence of quantum confinement effect. The UV photoluminescence is evidence of defect-free crystal formation and ban to band transition. The Tulshi extract aided ZnO nanorods showed excellent antimicrobial effect on *E. Coli* yielding the material of some potent biomedical applications.

ACKNOWLEDGEMENTS

The authors sincerely acknowledge UGC-DAE-CSR Kolkata center for various characterization facilities. The research facility of DST-FIST Programme of P. K. College, Contai is also highly acknowledged.

REFERENCES

1. P. Kambhampati, *J. Phys. Chem. Lett.* **12**, 4769 (2021) https://doi.org/10.1021/acs.jpclett.1c00754.
2. B. Mekuye, B. Abera, *Nano Select* **4**, 486 (2023) https://doi.org/10.1002/nano.202300038.
3. N. Baig, I. Kammakakam, W. Falath, *Mater. Adv.* **2**, 1821 (2021) https://doi.org/10.1039/D0MA00807A.
4. W.J. Song, *Talanta*, **170**, 74 (2017) https://doi.org/10.1016/j.talanta.2017.02.040.
5. M.S. Khan, V. Ranjan, A. Srivastava, *Proc.* – 2015 *IEEE Int. Symp. Nanoelectron. Inf. Syst. iNIS* 2015, 248 (2016).
6. F. Liu, C.C. Liu, K. Wu, F. Yang, Y. Yao, *Phys. Rev. Lett.*, **111**, 1 (2013) https://doi.org/10.1103/PhysRevLett.111.066804.
7. M.E. Davis, *Nature* **417**, 813 (2002) https://doi.org/10.1038/nature00785.
8. Y.H. Su, Y.F. Ke, S.L. Cai, Q.Y. Yao, *Light: Science & Applications* **1**, e14 (2012) https://doi.org/10.1038/lsa.2012.14.
9. V.N. Jafarova, G.S. Orudzhev, *Solid State Commun.* **325**, 114166 (2021) https://doi.org/10.1016/j.ssc.2020.114166.
10. H. Dong, B. Zhou, J. Li, J. Zhan, L. Zhang, *J. Materiomics* **3**, 255 (2017) https://doi.org/10.1016/j.jmat.2017.06.001.
11. S. Sahu, P.K. Samanta, *Materialstoday: Proc.* **65**, 2502 (2022) https://doi.org/10.1016/j.matpr.2022.04.474.
12. P.K. Samanta, M. Das, N.K. Rana, *J. Nano- Electron. Phys.* **11** No 1, 01028 (2019) https://doi.org/10.21272/jnep.11(1).01028.
13. J.A. Anta, E. Guillén, R. Tena-Zaera, *J. Phys. Chem. C* **116**, 11413 (2012) https://doi.org/10.1021/jp3010025.
14. B. Naiel, M. Fawzy, M.W.A. Halmy, A.E.D. Mahmoud, *Sci. Rep.* **12**, 20370 (2022) https://doi.org/10.1038/s41598-022-24805-2.
15. A. Fioravanti, P. Marani, S. Morandi, S. Lettieri, M. Mazzocchi, M. Sacerdoti, M.C. Carotta, *Sensors* **21**, 1331 (2021) https://doi.org/10.3390/s21041331.
16. P.K. Samanta, T. Kamilya, *J. Nanoeng. Nanomanuf.* **4**, 1 (2014) https://doi.org/10.1166/jnan.2014.1176.
17. Sukarman, B. Kristiawan, Khoirudin, A. Abdulah, K. Enoki, A.T. Wijayanta, *Nano-Structures & Nano-Objects* **38**, 101168 (2024) https://doi.org/10.1016/j.nanoso.2024.101168.
18. R.M.I. Elsamra, M.S. Masoud, A.A. Zidan, G.M.E. Zokm, M.A. Okbah, *Biomass Conversion and Biorefinery* **14**, 16843 (2024) https://doi.org/10.1007/s13399-022-03709-1.
19. A. Hymavathi, S. Nizamuddin, H. Bantikatla, *Materialstoday: Proc.* **54**, 557 (2022) https://doi.org/10.1016/j.matpr.2021.08.344.
20. G. Ghoshal, S. Sandal, *Food Chem. Adv.* **4**, 100702 (2024) https://doi.org/10.1016/j.focha.2024.100702.
21. P.K. Samanta, S. Datta, S. Basak, T. Kamilya, *Chem. Phys. Lett.* **584**, 155 (2013) https://doi.org/10.1016/j.cplett.2013.08.053.
22. P.K. Samanta, *Optik* **221**, 165337 (2020) https://doi.org/10.1016/j.ijleo.2020.165337.
23. J. Lv, C. Li, Z. Chai, *J. Lumin.* **208**, 225 (2019) https://doi.org/10.1016/j.jlumin.2018.12.050.

Структурні та оптичні властивості наностержнів ZnO, синтезованих за допомогою екстракту тулші (Ocimum tenuiflorum): екологічний підхід

K. Barman[1,2], P. Chakraborty[2], P.K. Samanta[3]

[1] *Department of Physics, Sri Ramkrishna Sarada Vidya Mahapitha, Hooghly-713102, West Bengal, India*
[2] *Department of Physics, Raiganj University, Uttar Dinajpur-733134, West Bengal, India*
[3] *Department of Physics, Prabhat Kumar College, Contai-721404, Purba Medinipur, West Bengal, India*

Для синтезу наностержнів ZnO з використанням екстракту Ocimum tenuiflorum було використано простий метод мокрої хімії. Дані рентгенівської дифракції показали утворення кристалічних наноструктур з розміром кристалітів ~ 18 нм. Наностержні мають полікристалічний характер і з'єднані між собою за допомогою електростатичного притягання між зарядженими гранями нанокристалів ZnO. Інфрачервоні спектри з перетворенням Фур'є виявили утворення зв'язку Zn-O разом з різними ароматичними зв'язками, також завдяки молекулам екстракту O.tenuiflorum. Спостерігалося сильне УФ-поглинання та випромінювання завдяки переходу краю зони прямої забороненої зони 3,85 еВ. Збільшення забороненої зони свідчить про наявність квантового обмеження в синтезованих наностержнях ZnO. Синтезовані наностержні демонструють сильну антимікробну активність проти E.coli, що було виявлено вимірюванням оптичної густини після інкубації бактерій з наностержнями.

Ключові слова: Оксид цинку, Зелений синтез, Поглинання, Заборонена зона, Квантове обмеження.